The dependence of the quark-meson model phase diagram on parameter fixing

Die Abhängigkeit des Quark-Meson-Modell Phasendiagramms von der Fixierung der Parameter
Bachelor-Thesis von Wael Elkamhawy
November 2014

TECHNISCHE
UNIVERSITÄT
DARMSTADT

Fachbereich Physik
Institut für Kernphysik
Nuclei, Hadrons and Quarks

The dependence of the quark-meson model phase diagram on parameter fixing
Die Abhängigkeit des Quark-Meson-Modell Phasendiagramms von der Fixierung der Parameter

Vorgelegte Bachelor-Thesis von Wael Elkamhawy

1. Gutachten: Priv. Doz. Dr. Michael Buballa
2. Gutachten: Prof. Dr. Jochen Wambach

Tag der Einreichung:

Abstract

The phase diagram of the quark-meson model is determined for different schemes of parameter fixing. For this purpose the thermodynamic potential for non-vanishing temperature and chemical potential is examined by applying the parameters resulting from different schemes. Within each scheme the parameter fixing is done in vacuum and the constituent quark mass in vacuum is set to 300 MeV, the pion decay constant to 88 MeV and the sigma meson mass to 600 MeV. The effects on the phase diagram caused by applying different schemes are studied and discussed. Two schemes lead to useful results while one is not physical.

Zusammenfassung

Das Quark-Meson-Modell Phasendiagramm wird für unterschiedliche Fixierungen der Parameter ermittelt. Hierfür wird das thermodynamische Potential für nicht verschwindende Temperatur und chemisches Potential mittels der in den unterschiedlichen Fixierungen erhaltenen Parameter untersucht. Alle Fixierungen werden im Vakuum durchgeführt und die Konstituentenquarkmasse wird auf 300 MeV, die Pionenzerfallskonstante auf 88 MeV und die Masse des Sigma-Mesons auf 600 MeV gesetzt. Die Effekte auf das Phasendiagramm durch die Anwendung verschiedener Fixierungen werden untersucht und diskutiert. Zwei der Fixierungen führen zu sinnvollen Ergebnissen, während eine unphysikalisch ist.

Erklärung zur Bachelor-Thesis

Hiermit versichere ich, die vorliegende Bachelor-Thesis ohne Hilfe Dritter nur mit den angegebenen Quellen und Hilfsmitteln angefertigt zu haben. Alle Stellen, die aus Quellen entnommen wurden, sind als solche kenntlich gemacht. Diese Arbeit hat in gleicher oder ähnlicher Form noch keiner Prüfungsbehörde vorgelegen.

Darmstadt, den 18. November 2014

_____

(Wael Elkamhawy)

Contents

1 Introduction

The physics of strong interacting particles, as quarks, is described by quantum chromodynamics (QCD). Those particles carry a colour charge and couple to the strong force which is mediated by gauge bosons, the so-called gluons. In contrast to the gauge bosons of the electromagnetic interaction, the photons, gluons also carry colour charge which makes the theory more complicated. A central phenomenon of QCD is confinement which postulates that only colour neutral particles are observable. This is realized in nature by quark-antiquark pairs, the mesons, or in three quark states, the baryons. Only at high temperatures or densities quarks and gluons are deconfined and form a so-called quark-gluon-plasma (QGP). The understanding of the quark-gluon-plasma is of big interest because it plays an important role in the development of the early universe and in densed matter as in neutron stars.

The determination of the QCD phase diagram is very difficult and still not fully understood. For this reason effective models reflecting the symmetries of the strong interaction are used to describe the low-energy sector of QCD. Those models include parameters which have to be fixed by observables but it is not clear without ambiguity in which way. Hence the phase diagram of the effective model depends on the scheme which is used to fix those parameters. This dependence of the phase diagram on parameter fixing is studied in this thesis by applying the renormalizable quark-meson model considering the two lightest quarks with flavour up and down. Due to global symmetries instead of local gauge symmetries within this model, the phenomenon of confinement cannot be described but it contains the important $SU_L(2) \otimes SU_R(2)$ symmetry of QCD in the limit of vanishing bare quark masses (chiral limit). We know, however, that the bare quark masses are finite but compared to hadronic scales they are very small such that the symmetry may be considered as an approximate symmetry of QCD. This symmetry is called the chiral symmetry and means that each component of the decomposed quark spinor, in particular decomposed in a left-handed and right-handed part by applying projection operators, transforms independently from one another. The phase diagram of the quark-meson model distinguishes between the chiral spontaneously broken phase and the chiral restored phase. In the spontaneously broken phase the quarks form a non-vanishing quark condensate and receive an effective quark mass, the so-called constituent quark mass.

The goal of this thesis is to analyse the dependence of the quark-meson model phase diagram on parameter fixing. Therefore the phase diagram is determined by applying different schemes of parameter fixing and finally the results are discussed.

2 Formalism

2.1 Conventions

Throughout this thesis natural units are used, meaning that the speed of light, Boltzmann constant and the reduced Planck constant are set to one

$$\hbar = c = k_B = 1 \ . \tag{2.1}$$

The units of physical quantities are then expressed in terms of units of energy. Furthermore Feynman slash notation, a short notation for a contraction, e.g.

$$\slashed{A} = \gamma_\mu A^\mu = \gamma^\mu A_\mu \ , \tag{2.2}$$

is used. Here γ_μ represents the gamma matrices known as the Dirac matrices.

2.2 The quark-meson model

The Lagrangian of the two-flavour quark-meson model in the chiral limit is given by

$$\mathscr{L}_{QM} = \bar{\psi} i \slashed{\partial} \psi - \bar{\psi} g \big(\sigma + i \gamma_5 \vec{\tau} \cdot \vec{\pi} \big) \psi + \mathscr{L}_M^{kin} - U(\sigma, \vec{\pi}) \ . \tag{2.3}$$

Here ψ denotes a $4 N_f N_c$-dimensional quark spinor with $N_f = 2$ flavour and $N_c = 3$ colour degrees of freedom, σ is the real scalar field of the sigma meson and $\vec{\pi}$ the real pseudo-scalar fields of the pion triplet. The first term describes the free Dirac Lagrangian for massless fermions (chiral limit), the second term their coupling to the sigma and pion fields. The third term represents the kinetic energies of the mesons and reads

$$\mathscr{L}_M^{kin} = \frac{1}{2} \big(\partial_\mu \sigma \partial^\mu \sigma + \partial_\mu \vec{\pi} \partial^\mu \vec{\pi} \big) \tag{2.4}$$

while the last term stands for the meson potential

$$U(\sigma, \vec{\pi}) = \frac{\lambda}{4} \big(\sigma^2 + \vec{\pi}^2 - v^2 \big)^2 \tag{2.5}$$

in which v is a parameter.

2.3 Symmetries

The introduced quark-meson Lagrangian exhibits a $SU_V(2) \otimes SU_A(2)$ symmetry which in chiral representation reads $SU_L(2) \otimes SU_R(2)$. This is the so-called chiral symmetry. The $SU_V(2)$ symmetry corresponds to the transformation

$$\Lambda_V : \psi \longrightarrow e^{-i\frac{\vec{\tau}}{2}\vec{\theta}}\psi$$
$$\bar{\psi} \longrightarrow \bar{\psi}e^{i\frac{\vec{\tau}}{2}\vec{\theta}} \,, \tag{2.6}$$

whereas the $SU_A(2)$ symmetry corresponds to the transformation

$$\Lambda_A : \psi \longrightarrow e^{-i\gamma_5\frac{\vec{\tau}}{2}\vec{\theta}}\psi$$
$$\bar{\psi} \longrightarrow \bar{\psi}e^{-i\gamma_5\frac{\vec{\tau}}{2}\vec{\theta}} \,. \tag{2.7}$$

The infinitesimal transformations are given by the series expansion of the exponential function to first order. Those expressions are then applied to determine the transformations of each term in the quark-meson Lagrangian. Since an infinitesimal transformation of the fields is considered, terms with second order in $\vec{\theta}$ are negligible. For the free Dirac Lagrangian we get

$$\Lambda_V : i\bar{\psi}\slashed{\partial}\psi \longrightarrow i\bar{\psi}\Big(1+i\frac{\vec{\tau}}{2}\vec{\theta}\Big)\slashed{\partial}\Big(1-i\frac{\vec{\tau}}{2}\vec{\theta}\Big)\psi = i\bar{\psi}\slashed{\partial}\psi \tag{2.8}$$

$$\Lambda_A : i\bar{\psi}\slashed{\partial}\psi \longrightarrow i\bar{\psi}\Big(1-i\gamma_5\frac{\vec{\tau}}{2}\vec{\theta}\Big)\slashed{\partial}\Big(1-i\gamma_5\frac{\vec{\tau}}{2}\vec{\theta}\Big)\psi$$
$$= i\Big[\bar{\psi}\slashed{\partial}\psi - i\vec{\theta}\Big(\bar{\psi}\frac{\vec{\tau}}{2}\gamma_5\gamma^\mu\partial_\mu\psi + \bar{\psi}\frac{\vec{\tau}}{2}\gamma^\mu\gamma_5\partial_\mu\psi\Big)\Big]$$
$$= i\bar{\psi}\slashed{\partial}\psi \,. \tag{2.9}$$

Hence the free Dirac Lagrangian is invariant under application of Λ_V and Λ_A. In the last step the relation $\{\gamma_5, \gamma^\mu\} = 0$ was used.
In order to find out how the meson fields transform under Λ_V and Λ_A, we consider combinations of the quark fields that carry the quantum numbers of the mesons

$$\text{pion-like state} : \vec{\pi} = i\bar{\psi}\vec{\tau}\gamma_5\psi \tag{2.10}$$

$$\text{sigma-like state} : \sigma = \bar{\psi}\psi \,. \tag{2.11}$$

Now the transformations can be applied to the quark fields in the meson-like states and using the relations $[\tau_j, \tau_k] = 2i\epsilon_{jkl}\tau_l$ and $\{\tau_j, \tau_k\} = 2\delta_{jk}\mathbb{1}_{\text{Flavour}}$ lead to

$$\Lambda_V : \vec{\pi} \longrightarrow \vec{\pi} + \vec{\theta} \times \vec{\pi}$$
$$\sigma \longrightarrow \sigma \tag{2.12}$$
$$\Lambda_A : \vec{\pi} \longrightarrow \vec{\pi} + \vec{\theta}\sigma$$
$$\sigma \longrightarrow \sigma - \vec{\theta}\vec{\pi} \,. \tag{2.13}$$

The squares of the fields transform as

$$\Lambda_V : \vec{\pi}^2 \longrightarrow \vec{\pi}^2$$
$$\sigma^2 \longrightarrow \sigma^2 \tag{2.14}$$
$$\Lambda_A : \vec{\pi}^2 \longrightarrow \vec{\pi}^2 + 2\sigma\vec{\theta}\vec{\pi}$$
$$\sigma^2 \longrightarrow \sigma^2 - 2\sigma\vec{\theta}\vec{\pi} . \tag{2.15}$$

Therefore the combination $\left(\vec{\pi}^2 + \sigma^2\right)$ is invariant under both transformations

$$\left(\vec{\pi}^2 + \sigma^2\right) \xrightarrow{\Lambda_V, \Lambda_A} \left(\vec{\pi}^2 + \sigma^2\right) . \tag{2.16}$$

The transformation of the derivatives of the meson fields is performed analogously and we get

$$\left(\partial_\mu\sigma\partial^\mu\sigma + \partial_\mu\vec{\pi}\partial^\mu\vec{\pi}\right) \xrightarrow{\Lambda_V, \Lambda_A} \left(\partial_\mu\sigma\partial^\mu\sigma + \partial_\mu\vec{\pi}\partial^\mu\vec{\pi}\right) . \tag{2.17}$$

As a result the meson potential $U(\sigma, \vec{\pi})$ and the kinetic energies of the mesons $\mathscr{L}_M^{kin}$ in the quark-meson Lagrangian are invariant under both transformations.
Identifying the pion-like and sigma-like states in the term describing the coupling of the fermions to the meson fields in the quark-meson Lagrangian,

$$\bar{\psi}g\left(\sigma + i\gamma_5\vec{\tau}\cdot\vec{\pi}\right)\psi , \tag{2.18}$$

shows that this term transforms as $g\left(\sigma^2 + \vec{\pi}^2\right)$ and hence it is also invariant under both transformations.
Altogether the quark-meson Lagrangian is invariant under $SU_V(2) \otimes SU_A(2)$ transformations.
Moreover a global phase transformation leaves the quark-meson Lagrangian invariant which reflects the $U_V(1)$ symmetry.
The full symmetry of the quark-meson Lagrangian reads

$$SU_V(2) \otimes SU_A(2) \otimes U_V(1) . \tag{2.19}$$

According to Noether's theorem all those continuous symmetries lead to conserved quantities. In this case the $SU_V(2)$ symmetry leads to the conserved vector current and analogously the $SU_A(2)$ symmetry leads to the conserved axial vector current [1] while the $U_V(1)$ symmetry is related to the conservation of the baryon number.

2.4 Spontaneous symmetry breaking

In case of invariances of the Lagrangian under given continuous symmetry transformations the ground state does not need to possess the same symmetries. In general it will show the same or less symmetries. The latter describes spontaneous symmetry breaking which is the essential part of Goldstone's theorem.

2.4.1 Goldstone's theorem

In order to apply Goldstone's theorem [2] to a certain theory or model the following three conditions have to be fulfilled:

1. Poincaré invariance (Lorentz invariance and additional invariance under linear translation in spacetime)

2. Existence of a conserved Noether current j_μ with $\partial^\mu j_\mu = 0$ which implies a continuous symmetry of the considered Lagrangian

3. The symmetry of the Noether charge Q may be spontaneously broken. That means that the ground state is not invariant under the action of the charge operator $Q\,|0\rangle \neq 0$

Goldstone's theorem then predicts a massless boson in the spectrum of the theory or model, the so-called Goldstone boson [3]. If the continuous symmetry is just an approximate symmetry, the boson receives a light mass and is called a pseudo-Goldstone boson [4].

We know that in nature the bare quark masses are finite but small compared to hadronic scales which results in a small explicit breaking of chiral symmetry. Due to small explicit breaking, the chiral symmetry may be considered as an approximate symmetry and hence we have pseudo-Goldstone bosons with light masses, the pions.

Since the explicit breaking of the chiral symmetry has no influence on the study in this thesis such part in the quark-meson Lagrangian is omitted and therefore the Lagrangian describes massless fermions, in particular the two lightest quarks with the flavours up and down.

If the model is in the spontaneously broken phase then the Goldstone bosons are given by the pion triplet and the expectation value of the sigma meson denoted by $\langle\sigma\rangle$ is not vanishing. When the Lagrangian is now expanded around this expectation value, the fermions appear with a mass term, the so-called constituent quark mass. Instead of expanding the quark-meson Lagrangian around the sigma meson expectation value, we could just replace the sigma meson field in the Lagrangian by its expectation value so we get a term

$$\bar\psi\big(i\slashed\partial - g\langle\sigma\rangle\big)\psi \;, \tag{2.20}$$

which describes fermions with a mass given by

$$M = g\langle\sigma\rangle \;. \tag{2.21}$$

This means that the spontaneous breakdown of chiral symmetry generates a fermion mass or in other words the fermions form a non-vanishing quark condensate.

2.5 Thermodynamic potential

In order to analyse the thermodynamic properties of the considered model it is necessary to derive an expression for the grand potential per Volume V

$$\Omega(T,\mu) = -\frac{T}{V}\log\mathscr{Z}(T,\mu) = -\frac{T}{V}\log\int\mathscr{D}\bar\psi\,\mathscr{D}\psi\,\mathscr{D}\sigma\,\mathscr{D}\vec\pi\,\exp\left(\int_{V_4} d^4x_E(\mathscr{L}_{QM} + \mu\bar\psi\gamma^0\psi)\right)[5]\;. \tag{2.22}$$

Here $\mathscr{Z}(T, \mu)$ denotes the grand canonical partition function depending on the temperature T and the quark chemical potential μ while the integral in the exponent is performed in Euclidean spacetime $x_E = (\tau, \vec{x})$ with the imaginary time $\tau = it$ and extends over the four-volume [5] $V_4 = [0, \frac{1}{T}] \times V$.

In mean-field approximation, in which the meson fields are replaced by their expectation values and so become classical fields, and in case of homogeneous fields, the quark energies can be expressed as

$$E_{\vec{p}} = \sqrt{\vec{p}^2 + g^2(\sigma^2 + \vec{\pi}^2)} \, [5] \tag{2.23}$$

and the thermodynamic potential then takes the form [5]

$$\Omega_{\text{hom}}(T, \mu; \sigma, \vec{\pi}) = -2N_f N_c \int \frac{d^3p}{(2\pi)^3} \left\{ E_{\vec{p}} + T \log\left[1 + e^{-\frac{E_{\vec{p}} - \mu}{T}} \right] + T \log\left[1 + e^{-\frac{E_{\vec{p}} + \mu}{T}} \right] \right\} + U(\sigma, \vec{\pi}) \,. \tag{2.24}$$

Due to the relation $M = g\langle\sigma\rangle$ the quark energies and thermodynamic potential can also be expressed via a new variable $m = g\sigma$ and hence we get for the energies

$$E_{\vec{p}} = \sqrt{\vec{p}^2 + m^2 + g^2\vec{\pi}^2} \tag{2.25}$$

and for the thermodynamic potential

$$\Omega_{\text{hom}}(T, \mu; \sigma, \vec{\pi}) = -2N_f N_c \int \frac{d^3p}{(2\pi)^3} \left\{ E_{\vec{p}} + T \log\left[1 + e^{-\frac{E_{\vec{p}} - \mu}{T}} \right] + T \log\left[1 + e^{-\frac{E_{\vec{p}} + \mu}{T}} \right] \right\} + U(m, \vec{\pi}). \tag{2.26}$$

The latter expression for the thermodynamic potential is used in chapter 5 to determine the phase diagram.

2.5.1 Vacuum ground state

For the determination of the vacuum ground state it is necessary to study the thermodynamic potential of the vacuum which is given by the thermodynamic potential itself in the $T = \mu = 0$-limit

$$\Omega_{\text{vac}}(\sigma, \vec{\pi}) = -2N_f N_c \int \frac{d^3p}{(2\pi)^3} \sqrt{\vec{p}^2 + g^2(\sigma^2 + \vec{\pi}^2)} + \frac{\lambda}{4} (\sigma^2 + \vec{\pi}^2 - v^2)^2 \,. \tag{2.27}$$

In order to obtain a vacuum state with positive parity the expectation value of the pseudo-scalar pion field with negative parity has to vanish while the sigma meson expectation value with positive parity is denoted by $\langle\sigma\rangle$ [6].

The necessary condition for the minimum is a vanishing derivative of the vacuum potential

$$\left. \frac{\partial \Omega_{\text{vac}}}{\partial \sigma} \right|_{\sigma=\langle\sigma\rangle, \vec{\pi}=0} = \left. \frac{\partial \Omega_{\text{vac}}}{\partial \pi^a} \right|_{\sigma=\langle\sigma\rangle, \vec{\pi}=0} = 0 \,, \tag{2.28}$$

where a represents a component of the pion field. The resulting equation is divided by $\langle\sigma\rangle$ such that the trivial solution $\langle\sigma\rangle = 0$ is excluded. This leads to the so-called gap equation

$$\lambda\left(\langle\sigma\rangle^2 - v^2\right) = 2N_f N_c g^2 \int \frac{d^3p}{(2\pi)^3} \frac{1}{\sqrt{\vec{p}^2 + g^2\langle\sigma\rangle^2}} \ . \tag{2.29}$$

Inserting equation (2.21) gives

$$\lambda\left(\frac{M^2}{g^2} - v^2\right) = 2N_f N_c g^2 \int \frac{d^3p}{(2\pi)^3} \frac{1}{\sqrt{\vec{p}^2 + M^2}} \ . \tag{2.30}$$

In the following the integral in equation (2.30) together with the factor $2N_f N_c$ is labelled L_1 and using the residue theorem it can also be written as

$$L_1 = 4iN_f N_c \int \frac{d^4p}{(2\pi)^4} \frac{1}{p^2 - M^2 + i\epsilon} = 2N_f N_c \int \frac{d^3p}{(2\pi)^3} \frac{1}{\sqrt{\vec{p}^2 + M^2}} \tag{2.31}$$

so the gap equation reads

$$\lambda\left(\frac{M^2}{g^2} - v^2\right) = g^2 L_1 \ , \tag{2.32}$$

which can be solved for v^2

$$v^2 = \frac{M^2}{g^2} - \frac{g^2 L_1}{\lambda} \ . \tag{2.33}$$

The quark loop L_1 is quadratically divergent and needs to be regularized in order to get a finite value (see section 3.4).

3 Meson masses

In this chapter different definitions of the meson masses are introduced.

3.1 Tree-level mass

The tree-level mass of the mesons is defined by the second derivative of the meson potential at the thermodynamic minimum

$$m_{j,t}^2 = \frac{\partial^2 U}{\partial \phi_j^2}\bigg|_{\sigma=\langle\sigma\rangle, \vec{\pi}=0} ,\qquad (3.1)$$

where the field ϕ_j stands for the sigma meson or the pion field depending on the index j.
This definition leads to masses which the mesons would have in the absence of the coupling to the Dirac sea quarks.
Using equation (2.33) leads to the following expressions

$$m_{\sigma,t}^2 = \lambda\left(3\frac{M^2}{g^2} - v^2\right) = 2\lambda\frac{M^2}{g^2} + g^2 L_1 \qquad (3.2)$$

$$m_{\pi,t}^2 = \lambda\left(\frac{M^2}{g^2} - v^2\right) = g^2 L_1 . \qquad (3.3)$$

For $L_1 \neq 0$ the pion has a non-vanishing mass which is in contradiction to Goldstone's theorem predicting massless Goldstone bosons. This error can be corrected by taking quark-antiquark polarization loops into account which results in a dressed massless pion.

3.2 Dressed pole mass

The determination of the pole masses requires propagators of the mesons because their masses are then defined by the implicit equation

$$D_j^{-1}(q^2 = m_j^2) = 0 . \qquad (3.4)$$

First the tree-level propagators with their corresponding tree-level masses are defined

$$iD_{j,t}(q^2) = \frac{i}{q^2 - m_{j,t}^2 + i\epsilon} \qquad (3.5)$$

which are then dressed with quark-antiquark polarization loops

$$-i\Pi_j(q^2) = -\int \frac{d^4 p}{(2\pi)^4} \,\mathrm{tr}\left[\Gamma_j iS_F(p+q)\Gamma_j iS_F(p)\right] , \qquad (3.6)$$

where

$$\Gamma_\sigma = \mathbb{1}_{\text{Dirac}} \otimes \mathbb{1}_{\text{Colour}} \otimes \mathbb{1}_{\text{Flavour}} \,, \tag{3.7}$$

$$\Gamma_{\pi^a} = i\gamma_5 \otimes \mathbb{1}_{\text{Colour}} \otimes \tau^a \tag{3.8}$$

and $S_F(p)$ is the quark propagator in Minkowski space

$$S_F(p) = \frac{1}{\not{p} - M + i\epsilon} \,. \tag{3.9}$$

Those self-energy loops are summed up in a geometrical series as illustrated in figure 3.1.
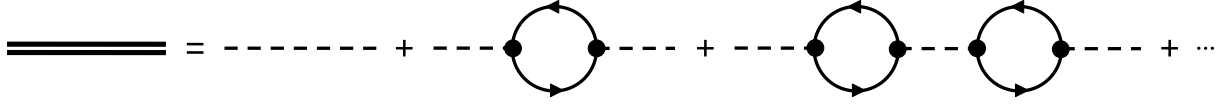

Figure 3.1.: The dressed meson propagator is given by a geometrical sum of quark-antiquark polarization loops and is indicated by a double line. The bare propagators are indicated by dashed lines while the filled circle stands for the Yukawa coupling g.

Now the dressed meson propagator reads

$$D_j(q^2) = \frac{1}{q^2 - m_{j,t}^2 + g^2 \Pi_j(q^2) + i\epsilon} \tag{3.10}$$

with its corresponding pole mass

$$m_j^2 = m_{j,t}^2 - g^2 \Pi_j(m_j^2) \,. \tag{3.11}$$

After evaluating the polarization loop (see Appendix A) the meson propagators read

$$D_\pi(q^2) = \frac{1}{q^2(1 - \frac{1}{2}g^2 L_2(q^2)) + i\epsilon} \tag{3.12}$$

$$D_\sigma(q^2) = \frac{1}{q^2 - \frac{1}{2}g^2(q^2 - 4M^2)L_2(q^2) - \frac{2\lambda M^2}{g^2} + i\epsilon} \,, \tag{3.13}$$

where the quark loop $L_2(q^2)$ using the residue theorem is given by

$$L_2(q^2) = 4iN_f N_c \int \frac{d^4 p}{(2\pi)^4} \frac{1}{[(p+q)^2 - M^2 + i\epsilon][p^2 - M^2 + i\epsilon]}$$

$$= 4N_f N_c \int \frac{d^3 p}{(2\pi)^3} \frac{1}{\sqrt{\vec{p}^2 + M^2}} \frac{1}{\left(q^2 - 4(\vec{p}^2 + M^2) + i\epsilon\right)} \,. \tag{3.14}$$

Hence the pion pole mass is now vanishing in consistency with Goldstone's theorem while the corresponding implicit equation for the determination of the sigma meson pole mass is given by

$$m_\sigma^2 - \frac{1}{2}g^2(m_\sigma^2 - 4M^2)L_2(m_\sigma^2) - \frac{2\lambda M^2}{g^2} = 0 \,. \tag{3.15}$$

3.2.1 Renormalized quark-meson coupling constant

If the polarization loop is expanded around the pole mass

$$\Pi_j(q^2) = \Pi_j(m_j^2) + \Pi'(m_j^2)(q^2 - m_j^2) + \dots \tag{3.16}$$

with

$$\Pi' = \frac{d}{dq^2}\Pi(q^2) \,, \tag{3.17}$$

the meson propagator in the vicinity of the pole can be written as

$$D_j(q^2) = \frac{Z_j}{q^2 - m_j^2 + i\epsilon} + \text{regular terms} \,, \tag{3.18}$$

where Z_j is the wave-function renormalization constant and is given by

$$Z_j = \frac{1}{1 + g^2\Pi_j'(m_j^2)} \,. \tag{3.19}$$

Figure 3.2.: Scattering of two quarks by an exchange of a dressed meson.

Considering the scattering of two quarks by an exchange of a dressed meson as depicted in figure 3.2 leads to the expression

$$g^2 D_j(q^2) = g^2 \frac{Z_j}{q^2 - m_j^2 + i\epsilon} = \frac{g_j^2}{q^2 - m_j^2 + i\epsilon} \tag{3.20}$$

which gives the renormalized quark-meson coupling constant at the pole

$$g_j = g\sqrt{Z_j} \,. \tag{3.21}$$

This expression can now be used to determine the renormalized quark-meson coupling constant in the vicinity of the pole

$$g_\pi^2 = g^2 Z_\pi = g^2 D_\pi(m_\pi^2)(q^2 - m_\pi^2) = g^2 D_\pi(0)q^2 = \frac{g^2}{1 - \frac{1}{2}g^2 L_2(0)} \,. \tag{3.22}$$

3.3 Screening mass

Analogously to the definition of the tree-level mass, the screening meson mass is defined by the curvature of the thermodynamic potential instead of the meson potential and is also evaluated at the thermodynamic minimum, e.g. in vacuum

$$m_{j,s}^2 = \left.\frac{\partial^2 \Omega_{\text{vac}}}{\partial \phi_j^2}\right|_{\sigma=\langle\sigma\rangle,\vec{\pi}=0} . \tag{3.23}$$

Using the definition of the screening mass, the gap-equation solved for v^2 given by equation (2.33) and the relation $M = g\langle\sigma\rangle$ leads to the expression

$$m_{\sigma,s}^2 = 2\lambda \frac{M^2}{g^2} + 2g^2 M^2 N_f N_c \int \frac{d^3 p}{(2\pi)^3} \frac{1}{\sqrt{\vec{p}^2 + M^2}^3} , \tag{3.24}$$

so the sigma meson screening mass reads

$$m_{\sigma,s}^2 = 2\lambda \frac{M^2}{g^2} - 2g^2 M^2 L_2(0) . \tag{3.25}$$

For the pion meson mass we obtain

$$m_{\pi^a}^2 = \left.\frac{\partial^2 \Omega_{\text{vac}}}{\partial(\pi^a)^2}\right|_{\sigma=\langle\sigma\rangle,\vec{\pi}=0} = -g^2 L_1 + \lambda\left(\langle\sigma\rangle^2 - v^2\right) . \tag{3.26}$$

Now using the gap equation solved for v^2 given by equation (2.33) and the relation $M = g\langle\sigma\rangle$ gives

$$m_{\pi^a}^2 = -g^2 L_1 + \lambda\left(\frac{M^2}{g^2} - \frac{M^2}{g^2} + \frac{g^2 L_1}{\lambda}\right) = 0 . \tag{3.27}$$

Hence the pion screening mass is vanishing. This is in consistency with Goldstone's theorem.

3.4 Regularization

In order to remove the quadratic divergence in the quark loop L_1, the logarithmic divergence in $L_2(q^2)$ and the quartic divergence in the thermodynamic potential a regularization is needed. In this thesis the standard Pauli-Villars regularization scheme [7] is used with three regulating functions

$$\int \frac{d^3p}{(2\pi)^3} F(M^2) \longrightarrow \int \frac{d^3p}{(2\pi)^3} \sum_{j=0}^{3} c_j F(M^2 + j\Lambda^2) \tag{3.28}$$

with a cutoff parameter Λ and the coefficients $c_0 = 1$, $c_1 = -3$, $c_2 = 3$ and $c_3 = -1$. Those regulating functions have the same asymptotic behaviour as the original such that they cancel out each other for asymptotic momenta by subtracting themselves.

The number of regulating functions needed to ensure convergence increases by increasing the degree of divergence.

4 Parameter fixing

In this chapter different schemes of parameter fixing for determination of the parameters λ, g^2 and v^2 are introduced. The calculations within each scheme are done in vacuum. They differ from one another by using different relations but the same given data, the constituent quark mass in vacuum $M = 300$ MeV, the pion decay constant $f_\pi = 88$ MeV and the sigma meson mass given by $2M$. It is not specified which of the introduced sigma meson mass is set to $2M$.

4.1 Standard mean-field approximation

The thermodynamic potential in vacuum given by equation (2.27) includes a divergent integral. In order to handle this divergence we could regularize the integral or just omit it. The latter is done in standard mean-field approximation (sMFA) and therefore the thermodynamic potential in vacuum is just given by the meson potential

$$\Omega_{\text{vac}}^{\text{sMFA}}(\sigma, \vec{\pi}) = U(\sigma, \vec{\pi}) = \frac{\lambda}{4}\left(\sigma^2 + \vec{\pi}^2 - v^2\right)^2 . \tag{4.1}$$

The gap equation solved for v^2 given by equation (2.33) simplifies to

$$v^2 = \frac{M^2}{g^2} . \tag{4.2}$$

Using the Goldberger-Treiman relation [5]

$$M = g_\pi f_\pi \tag{4.3}$$

and the fact that in sMFA the quark-meson coupling constant is equal to the bare Yukawa coupling g, the parameter g is fixed by

$$g = \frac{M}{f_\pi} . \tag{4.4}$$

Inserting the result for g into equation (4.2) yields

$$v^2 = f_\pi^2 . \tag{4.5}$$

The meson masses in sMFA are given by the tree-level masses and because the divergent integral in the thermodynamic potential is omitted, the divergent integral L_1 in the tree-level masses given by equation (3.2) and (3.3) does not occur and we obtain

$$m_{\sigma,t}^2 = 2\lambda\frac{M^2}{g^2} \tag{4.6}$$

$$m_{\pi,t}^2 = 0 . \tag{4.7}$$

Hence the pion mass is vanishing which is in consistency with Goldstone's theorem. Now the parameter λ can be fixed by setting the sigma meson mass to $2M$

$$\lambda = \frac{2M^2}{f_\pi^2} . \tag{4.8}$$

All parameters are now fixed and the phase diagram can be analysed by applying the results to the thermodynamic potential. This will be done in chapter 5.

4.2 First scheme of parameter fixing

The first scheme of parameter fixing uses the Goldberger Treiman relation [5]

$$M = g_\pi f_\pi \,, \tag{4.9}$$

the renormalized quark-meson coupling constant in the vicinity of the pole

$$g_\pi^2 = \frac{g^2}{1 - \frac{1}{2}g^2 L_2(0)} \tag{4.10}$$

and the gap equation solved for v^2

$$v^2 = \frac{M^2}{g^2} - \frac{g^2 L_1}{\lambda} \,. \tag{4.11}$$

Furthermore the dressed pole mass of the sigma meson is set to $2M$.
By using equation (4.9) and (4.10), the parameter g^2 can be fixed to

$$g^2 = \frac{M^2}{f_\pi^2 + \frac{1}{2}M^2 L_2(0)} \,. \tag{4.12}$$

Due to the fact that $L_2(0)$ depends on the cutoff parameter Λ the parameter g^2 also depends on Λ as shown in figure 4.1.
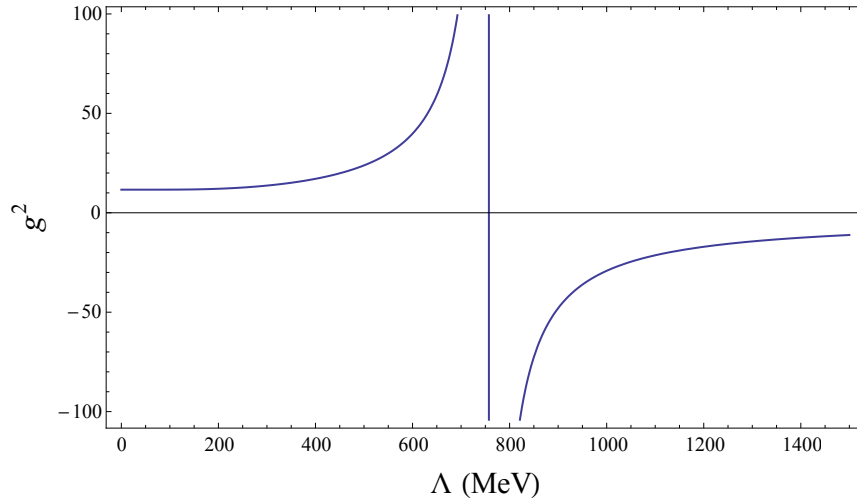

Figure 4.1.: Dependence of the parameter g^2 on Λ using the first scheme of parameter fixing.

As mentioned above, the pole mass of the sigma meson is set to $2M$ which is then inserted into equation (3.15) and hence the parameter λ is given by

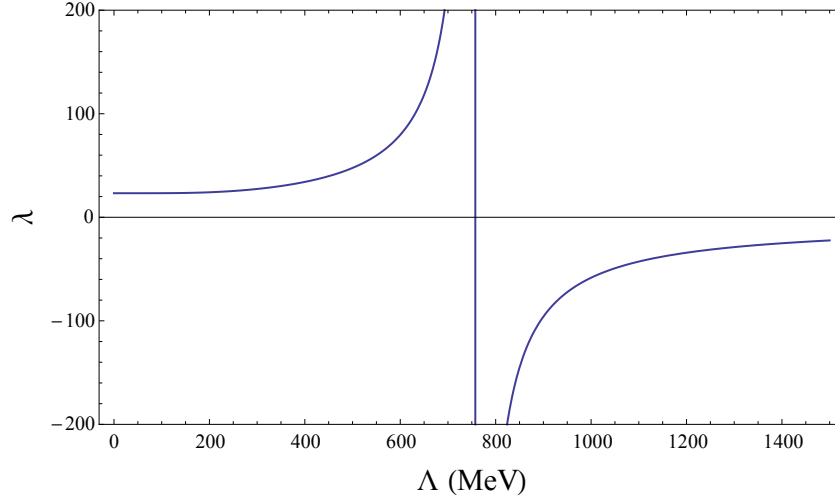$$\lambda = 2g^2 = \frac{2M^2}{f_\pi^2 + \frac{1}{2}M^2 L_2(0)} \,. \tag{4.13}$$

Figure 4.2.: Dependence of the parameter λ on Λ using the first scheme of parameter fixing.

The results for g^2 and λ are then inserted into equation (4.11) and we obtain

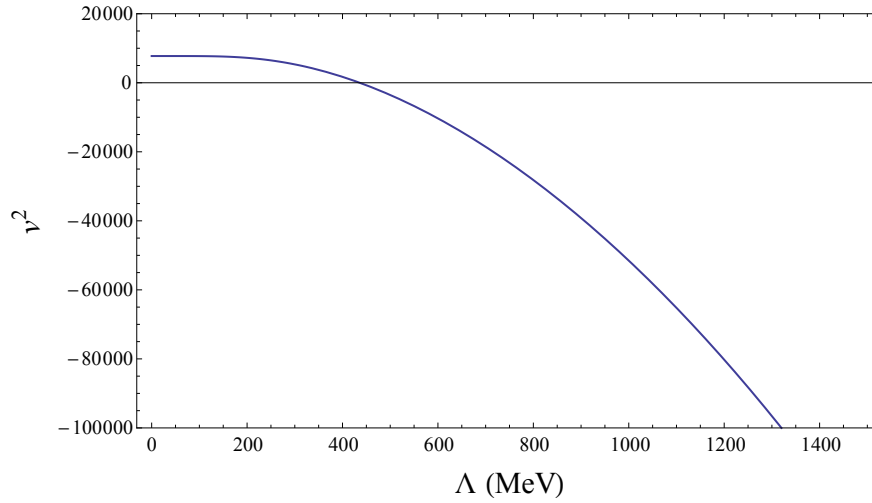$$v^2 = f_\pi^2 + \frac{1}{2}M^2 L_2(0) - \frac{1}{2}L_1 \,. \tag{4.14}$$

Figure 4.3.: Dependence of the parameter v^2 on Λ using the first scheme of parameter fixing.

4.3 Second scheme of parameter fixing

The second scheme of parameter fixing is quite similar to the first one which in particular means that all relations in the first scheme are also used in this one but now the screening sigma meson mass instead of the dressed pole mass is set to $2M$.

Using again the Goldberger Treiman relation and the renormalized quark-meson coupling constant in the vicinity of the pole yields once more

$$g^2 = \frac{M^2}{f_\pi^2 + \frac{1}{2}M^2 L_2(0)} \,. \tag{4.15}$$

The dependence of the parameter g^2 on the cutoff parameter Λ is already depicted in figure 4.1. As mentioned above now the sigma meson screening mass given by equation (3.25) is set to $2M$ which is then solved for λ

$$
\begin{aligned}
\lambda &= g^2\big(2 + g^2 L_2(0)\big) \\
&= \frac{M^2}{f_\pi^2 + \frac{1}{2}M^2 L_2(0)}\left(2 + \frac{M^2 L_2(0)}{f_\pi^2 + \frac{1}{2}M^2 L_2(0)}\right).
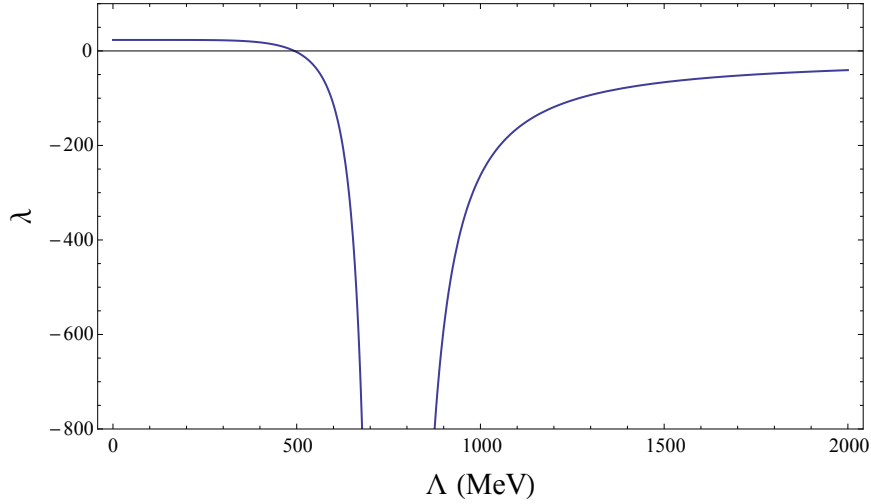\end{aligned}
\tag{4.16}
$$

Figure 4.4.: Dependence of the parameter λ on Λ using the second scheme of parameter fixing.

Inserting those two parameters into equation (2.33) fixes the parameter v^2

$$
v^2 = f_\pi^2 + \frac{1}{2}M^2 L_2(0) - \frac{L_1}{4}\frac{2f_\pi^2 + M^2 L_2(0)}{f_\pi^2 + M^2 L_2(0)} .
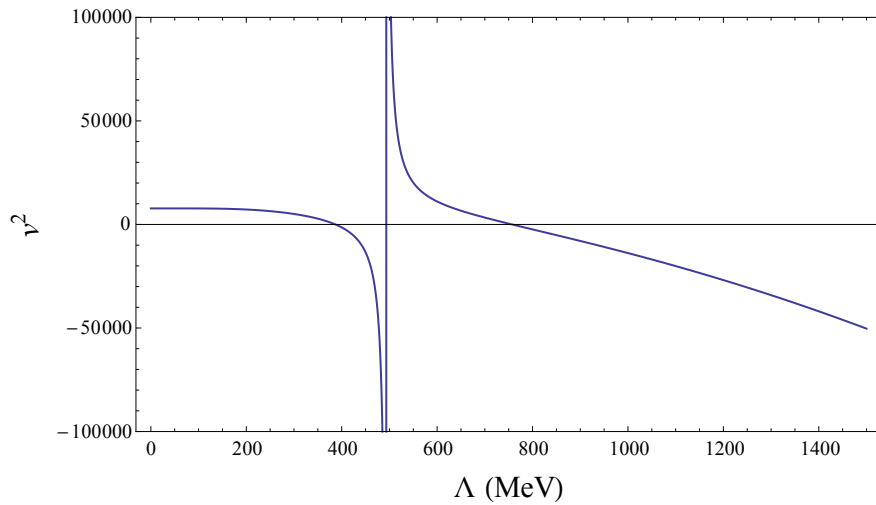\tag{4.17}
$$

Figure 4.5.: Dependence of the parameter v^2 on Λ using the second scheme of parameter fixing.

4.4 Third scheme of parameter fixing

The third scheme of parameter fixing sets the expectation value of the sigma meson field to f_π

$$\langle \sigma \rangle = f_\pi \,, \tag{4.18}$$

which is then used to fix g with equation (2.21)

$$g = \frac{M}{f_\pi} \,. \tag{4.19}$$

In this scheme g is independent of Λ.
The sigma meson screening mass is set to $2M$ which yields

$$\begin{aligned}
\lambda &= g^2 \big(2 + g^2 L_2(0)\big) \\
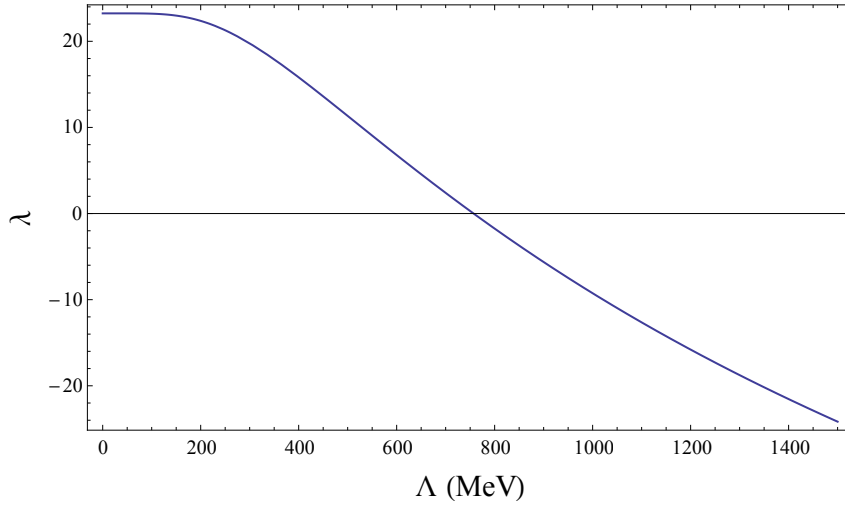&= \frac{M^2}{f_\pi^2} \left(2 + \frac{M^2}{f_\pi^2} L_2(0)\right).
\end{aligned} \tag{4.20}$$

Figure 4.6.: Dependence of λ on Λ using the third scheme of parameter fixing.

The parameter v^2 is fixed by using the gap equation and inserting the determined expressions for g and λ gives

$$v^2 = f_\pi^2 \left(1 - \frac{L_1}{2f_\pi^2 + M^2 L_2(0)}\right). \tag{4.21}$$
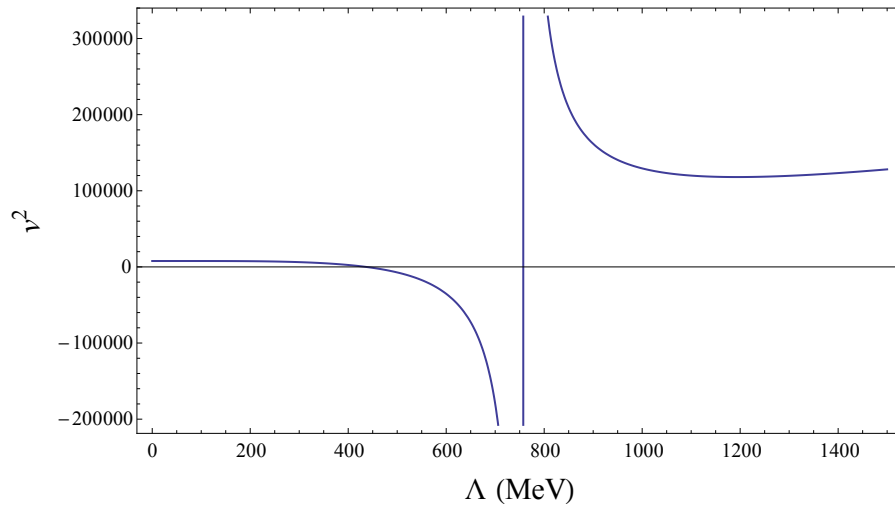
Figure 4.7.: Dependence of v^2 on Λ using the third scheme of parameter fixing.

5 Phase diagram

The phase diagram visualizes the boundary between different phases. In this case the two phases are the spontaneously broken phase of the chiral symmetry and the chiral restored phase. In the spontaneously broken phase the expectation value of the sigma meson field has a non-vanishing value and hence the constituent quark mass M is finite while in the restored phase the expectation value vanishes and so does the constituent quark mass. The expectation value of the sigma meson field represents the physical ground state of the model which means its value is determined by minimizing the thermodynamic potential with respect to the sigma meson field. In order to find this minimum the numerically determined thermodynamic potential depending on the sigma meson field is examined. Due to the linear relation between the sigma meson field and the mass m, the potential can be expressed as a function of m which is already done in equation (2.26).

The thermodynamic potential for $\Lambda = 300$ MeV, $\mu = 100$ MeV and $T = 50$ MeV is depicted in figure 5.1.
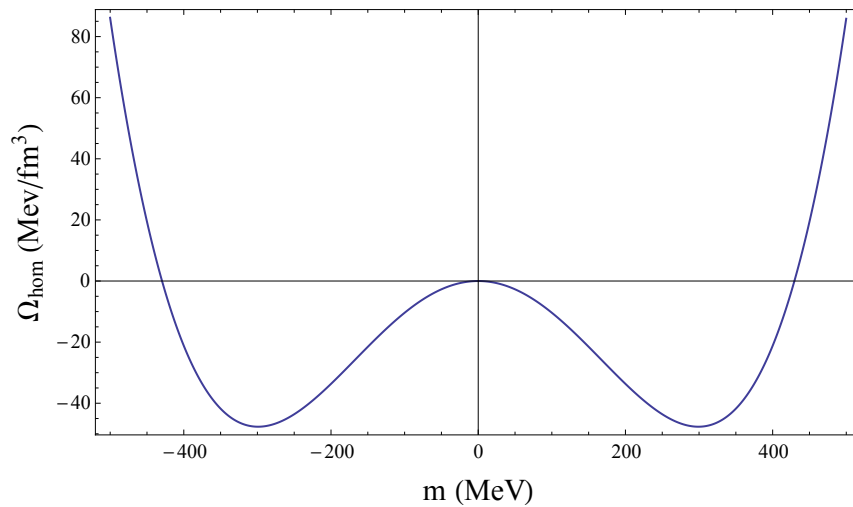

Figure 5.1.: Thermodynamic potential for $\Lambda = 300$ MeV, $\mu = 100$ MeV and $T = 50$ MeV.

Obviously the constituent quark mass M, given by the mass m in the minimum of the potential, has a finite value and hence the physical state for this combination of temperature T and chemical potential μ is in the spontaneously broken phase. By increasing the temperature, the chemical potential or both a phase transition to the chiral restored phase can emerge. This phase transition can happen in two different ways.

A first-order phase transition is characterized by a jumping value of the constituent quark mass M. This means that by increasing the temperature or the chemical potential, the position of the global minimum in the thermodynamic potential is jumping.
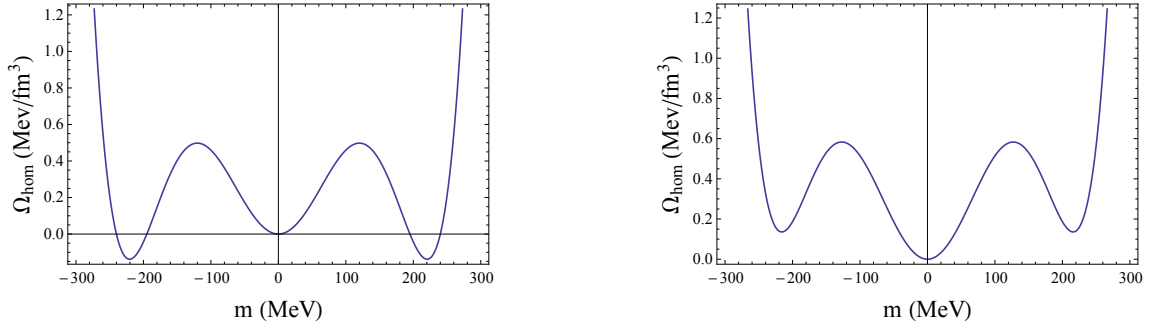
Figure 5.2.: Thermodynamic potential for $\Lambda = 300$ MeV, $\mu = 250$ MeV and $T = 68.3$ MeV (left) and $T = 68.9$ MeV (right). The local minimum at $m = 0$ MeV in the left diagram becomes a global minimum on the right diagram by increasing the temperature which is then the physical state. This illustrates a first-order phase transition.

In figure 5.2 the thermodynamic potential during a phase transition of first order is depicted. The constituent quark mass M is jumping from a finite value to zero.

A second-order phase transition is characterized by a continuous transition of the constituent quark mass M which means that the position of the global minimum changes continuously by varying the temperature or chemical potential.
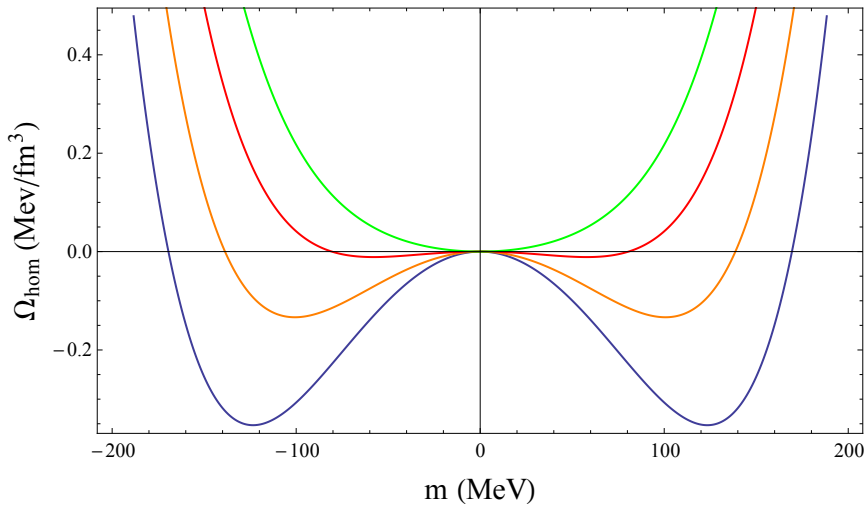

Figure 5.3.: Thermodynamic potential for $\Lambda = 300$ MeV and $\mu = 100$ MeV. From bottom to top the temperature increases $T = 137$ MeV, $T = 138$ MeV, $T = 139$ MeV, $T = 140$ MeV. For $T = 140$ MeV the constituent quark mass is zero and hence the system is in the chiral restored phase. This illustrates a second-order phase transition.

In figure 5.3 the thermodynamic potential during a phase transition of second order is shown. The so-called tricritical point in the phase diagram separates the first-order from second-order phase transition.

5.1 Phase diagram using the first scheme of parameter fixing

The results for the parameters of the first scheme are now used to determine the phase diagram by examining the thermodynamic potential given by equation (2.26) at non-vanishing temperature and chemical potential.
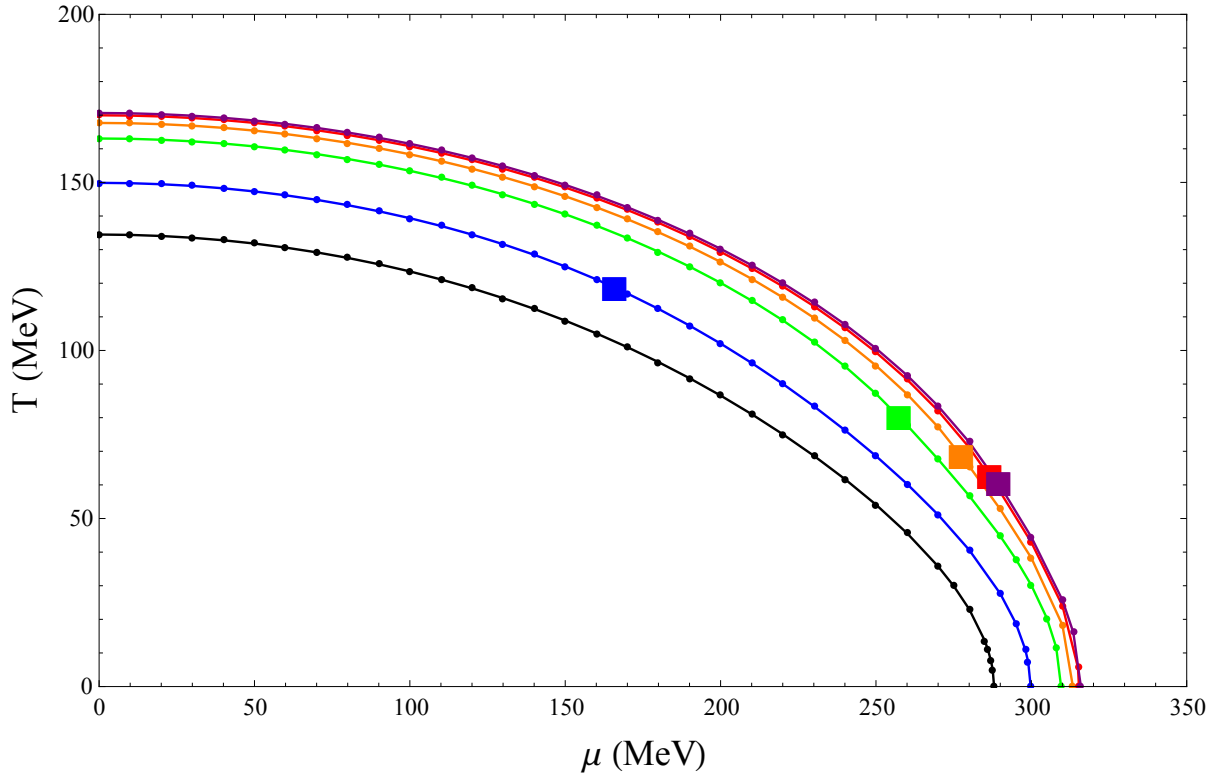

Figure 5.4.: The black line indicates the phase diagram in sMFA while the coloured lines include the Dirac sea using Pauli-Villars regularization with different values of the cutoff: $\Lambda = 300$ MeV, 600 MeV, 1 GeV, 2 GeV, 5 GeV (from bottom to top). The squares mark the tricritical points which separate second-order (to the left) from first-order (to the right) phase transitions. In sMFA it is always a first-order transition.

As shown in figure 5.4 there exists no trictritical point in sMFA. The phase transition along the entire phase boundary exhibits a first-order phase transition. This behaviour in the chiral limit and without the Dirac sea contribution, even at vanishing chemical potential [8, 9], is well known. This problem was carefully analyzed in Ref. [10] and was identified as an artifact of the standard mean-field approximation. For all other phase diagrams shown in figure 5.4 a trictritical point exists, separating the second-order from first-order phase transition.

The phase diagrams converge to one diagram by increasing the cutoff parameter Λ and also the tricritical points are approaching each other and finally they basically overlap. This behaviour reflects the renormalizable character of the model. The phase diagram for $\Lambda = 5$ GeV can be interpreted as "renormalized".

Though the phase diagrams show a renormalizable character, the thermodynamic potential is getting unstable if the parameter λ changes its sign which is expected according to equation (2.26). As a result the thermodynamic potential for $\Lambda = 757$ MeV or higher is not bounded from below and hence there is no physical ground state.
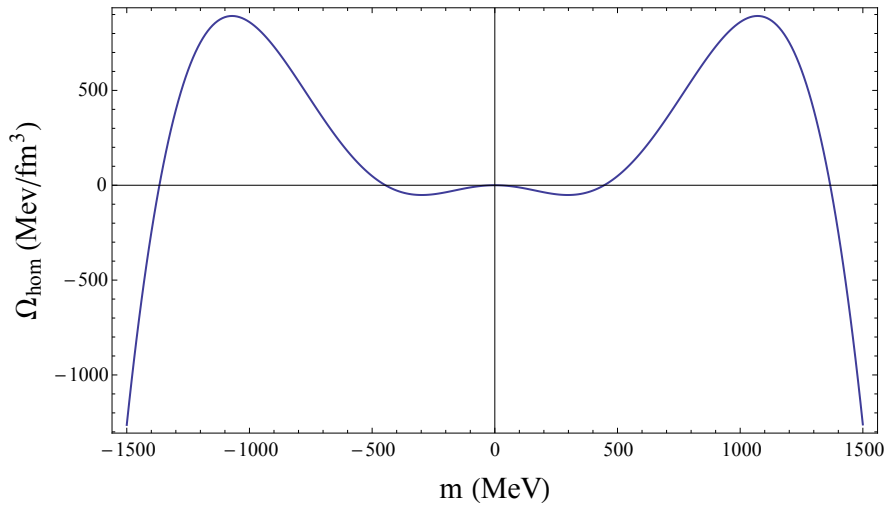
Figure 5.5.: Unstable thermodynamic potential for $\Lambda = 1000$ MeV, $\mu = 150$ MeV and $T = 50$ MeV.

5.2 Phase diagram using the second scheme of parameter fixing

Following, the parameters from the second scheme of parameter fixing are applied to determine the phase diagram.

As shown in figure 5.6 the phase diagrams for increasing cutoff parameter Λ collapse into the origin and for $\Lambda = 1330$ MeV and higher there are no phase diagrams because only the chiral restored phase is present.

Moreover for $\Lambda = 494$ MeV the parameter λ gets negative and hence the thermodynamic potential is getting unstable.

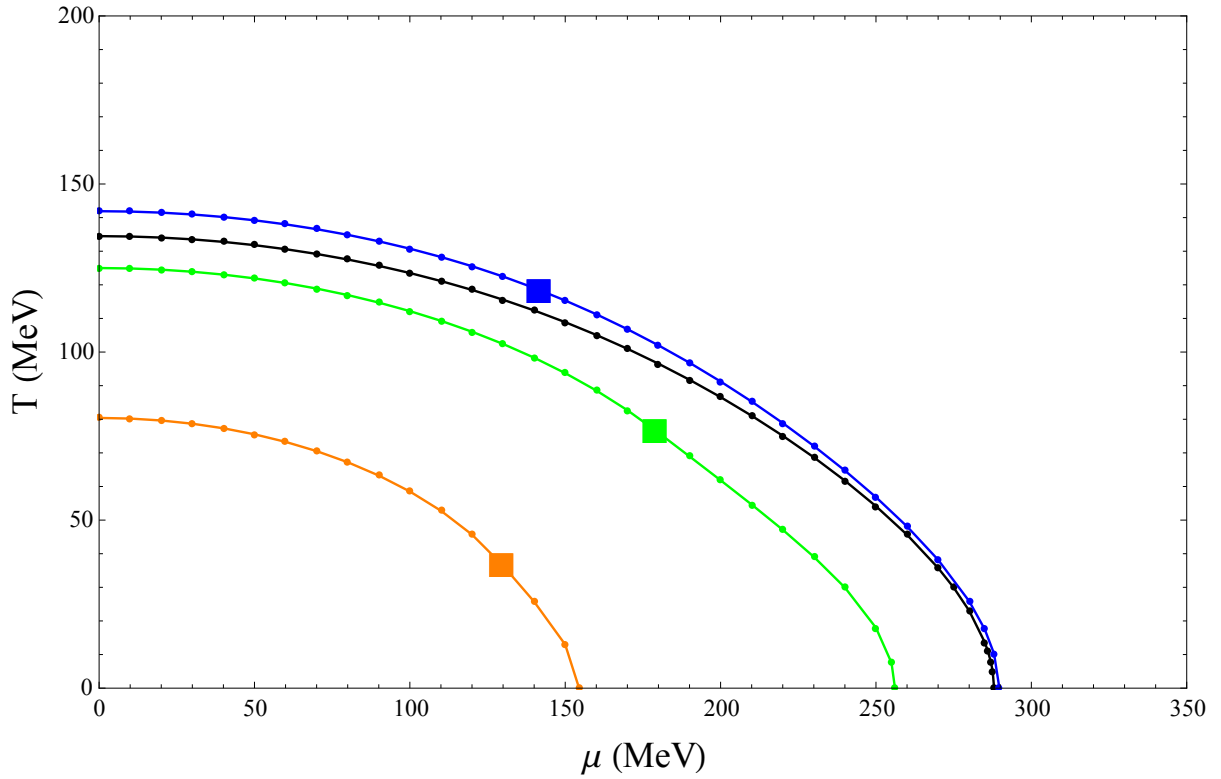**Figure 5.6.:** The black line indicates the phase diagram in sMFA while the coloured lines include the Dirac sea using Pauli-Villars regularization with different values of the cutoff: $\Lambda =$ 300 Mev, 600 MeV, 1 GeV (blue, green, orange). The squares mark the tricritical points which separate second-order (to the left) from first-order (to the right) phase transitions. In sMFA it is always a first-order transition.

5.3 Phase diagram using the third scheme of parameter fixing

Again the phase diagrams are determined, in this case using the parameters resulting from the third scheme.

Remarkably, all phase diagrams using the third scheme are completely identical to the phase diagrams based on the first scheme although the parameters in both schemes differ from one another.

On closer examination of the thermodynamic potential by inserting the parameters of each scheme, it is found that the analytic expressions are indeed the same which explains the same results. The only term in the thermodynamic potential given by equation (2.26) which is depending on the parameters is the meson potential. Therefore it is sufficient to compare the results of the meson potential using the parameters of each scheme.

Applying the first scheme in the meson potential and exploiting that the pion field in the minimum vanishes, which means that terms with $\vec{\pi}$ can be omitted, yields

$$U(m) = \frac{\lambda}{4}\left[\frac{m^2}{g^2} - v^2\right]^2 = \frac{M^2}{\left(2f_\pi^2 + M^2 L_2(0)\right)}\left[\frac{m^2\left(f_\pi^2 + \frac{1}{2}M^2 L_2(0)\right)}{M^2} - f_\pi^2 - \frac{1}{2}M^2 L_2(0) + \frac{L_1}{2}\right]^2$$
$$= \frac{M^2}{\left(2f_\pi^2 + M^2 L_2(0)\right)}\left[f_\pi^2\left(\frac{m^2}{M^2} - 1\right) + \left(\frac{m^2 - M^2}{2}\right)L_2(0) + \frac{L_1}{2}\right]^2. \tag{5.1}$$

Now applying the third scheme in the meson potential yields

$$U(m) = \frac{\lambda}{4}\left[\frac{m^2}{g^2} - v^2\right]^2 = \frac{\frac{M^2}{f_\pi^2}\left(2 + \frac{M^2}{f_\pi^2}L_2(0)\right)}{4}\left[\frac{m^2 f_\pi^2}{M^2} - f_\pi^2 + \frac{L_1 f_\pi^2}{\left(2f_\pi^2 + M^2 L_2(0)\right)}\right]^2$$
$$= \frac{\frac{M^2}{f_\pi^2}\left(2 + \frac{M^2}{f_\pi^2}L_2(0)\right)}{4}\left[\frac{2f_\pi^2}{\left(2f_\pi^2 + M^2 L_2(0)\right)}\frac{\left(\frac{m^2}{M^2} - 1\right)\left(2f_\pi^2 + M^2 L_2(0)\right) + L_1}{2}\right]^2$$
$$= \frac{1}{4}\frac{M^2}{f_\pi^2}\left(2 + \frac{M^2}{f_\pi^2}L_2(0)\right)\frac{4f_\pi^4}{\left(2f_\pi^2 + M^2 L_2(0)\right)^2}\left[f_\pi^2\left(\frac{m^2}{M^2} - 1\right) + \left(\frac{m^2 - M^2}{2}\right)L_2(0) + \frac{L_1}{2}\right]^2$$
$$= \frac{M^2}{\left(2f_\pi^2 + M^2 L_2(0)\right)}\left[f_\pi^2\left(\frac{m^2}{M^2} - 1\right) + \left(\frac{m^2 - M^2}{2}\right)L_2(0) + \frac{L_1}{2}\right]^2. \tag{5.2}$$

Comparing equation (5.1) with (5.2) shows that the meson potential applying the first and third scheme is indeed identical and hence the thermodynamic potential is identical which results in equal phase diagrams.

The thermodynamic potential is again getting unstable if the parameter λ changes its sign. Although the parameter λ differs from the one based on the first scheme, the change of sign takes place for $\Lambda = 757$ MeV and hence the thermodynamic potential is also not bounded from below for $\Lambda = 757$ MeV or higher.

6 Conclusion and outlook

In this thesis the phase diagram of the quark-meson model was determined for different schemes of parameter fixing by examining the thermodynamic potential.

First we just omitted the divergent term in the vacuum thermodynamic potential which corresponds to the so-called standard mean-field approximation. Due to the fact that no regularization including a cutoff parameter is needed, there is no dependence of the parameters on such a cutoff parameter. The phase transition in standard mean-field approximation exhibits a first-order transition along the entire phase boundary which is an artifact of the standard mean-field approximation.

The next step was to take the Dirac sea into account to receive more precise results. Therefore the divergent term in the vacuum thermodynamic potential is not omitted and hence the divergence has to be handled in a proper way. For this reason a regularization including a cutoff parameter Λ, in particular the Pauli-Villars regularization scheme, was used. In contrast to the parameters in standard mean-field approximation, the parameters now depend on such a cutoff parameter Λ. Since it is not clear without ambiguity how the parameters have to be fixed, three different schemes of parameter fixing are introduced.

The phase diagrams using the first and third scheme converge to one diagram for increasing cutoff parameter Λ which reflects the renormalizability of the model. This means that for arbitrarily high cutoff parameter, the phase diagrams will differ insignificantly from the one calculated for $\Lambda = 5$ GeV.

This behaviour does not occur in the phase diagrams by applying the second scheme of parameter fixing. Those diagrams collapse into the origin by increasing the cutoff parameter and for higher cutoff parameter than $\Lambda = 1330$ MeV only the chiral restored phase exists. Since it is well known that quarks in nature have a constituent quark mass of about 300 MeV in vacuum, they have to exist in the spontaneously broken phase in vacuum. This fact is in contradiction to the results for $\Lambda = 1330$ MeV or higher.

Though the phase diagram by applying the first and third scheme of parameter fixing converge to one diagram by increasing the cutoff parameter, the thermodynamic potential is not stable for arbitrary values of Λ. In particular for a cutoff parameter of $\Lambda = 757$ MeV or higher the parameter λ is negative. The thermodynamic potential is not bounded from below any more and hence there is no physical ground state for $\Lambda = 757$ MeV or higher.

Analogously the thermodynamic potential using the second scheme of parameter fixing is getting unstable for $\Lambda = 494$ MeV due to the change of sign of the parameter λ.

In contrast to the phase diagrams applying the first and third scheme of parameter fixing, the phase diagrams using the second scheme are not converging to a non-trivial diagram. The reason for this non-renormalizable character could be the fact that the sigma meson screening mass is used within this scheme, which in comparison to the pole mass is no good observable. This is a prerequisite for renormalization.

Altogether the second scheme of parameter fixing is not very physical since it is only applicable until $\Lambda = 494$ MeV and because the phase diagrams do not show a renormalizable character which means that the phase diagrams do not converge to one diagram.

The first and third scheme of parameter fixing are applicable until $\Lambda = 757$ MeV and in contrast to the second scheme the phase diagrams show a renormalizable character. Both schemes lead to the same homogeneous phase diagram but since the third scheme is using the sigma meson screening mass instead of the observable pole mass, the first scheme seems to be the more physical one. In order to extract visible differences between both schemes, we should examine the phase diagrams in inhomogeneous phases.

To remove instabilities in the thermodynamic potential based on each scheme of parameter fixing, we can study the phase diagram beyond mean-field approximation.

A Quark-antiquark polarization loops

The expressions for the quark-antiquark polarization loops are given by

$$-i\Pi_j(q^2) = -\int \frac{d^4p}{(2\pi)^4} \, \mathrm{tr}\left[\Gamma_j iS_F(p+q)\Gamma_j iS_F(p)\right] \tag{A.1}$$

with

$$\Gamma_\sigma = \mathbb{1}_{\mathrm{Dirac}} \otimes \mathbb{1}_{\mathrm{Colour}} \otimes \mathbb{1}_{\mathrm{Flavour}}, \tag{A.2}$$

$$\Gamma_{\pi^a} = i\gamma_5 \otimes \mathbb{1}_{\mathrm{Colour}} \otimes \tau^a \tag{A.3}$$

and

$$S_F(p) = \frac{1}{\not{p} - M + i\epsilon} = \frac{(\not{p} + M)}{p^2 - M^2 + i\epsilon'}. \tag{A.4}$$

For the sigma meson we obtain [11]

$$
\begin{aligned}
-i\Pi_\sigma(q^2) &= -\int \frac{d^4p}{(2\pi)^4} \, \mathrm{tr}\left[\mathbb{1}_{\mathrm{Dirac}} \otimes \mathbb{1}_{\mathrm{Colour}} \otimes \mathbb{1}_{\mathrm{Flavour}} iS_F(p+q)\mathbb{1}_{\mathrm{Dirac}} \otimes \mathbb{1}_{\mathrm{Colour}} \otimes \mathbb{1}_{\mathrm{Flavour}} iS_F(p)\right] \\
&= \int \frac{d^4p}{(2\pi)^4} \, \mathrm{tr}\left[\mathbb{1}_{\mathrm{Dirac}} \otimes \mathbb{1}_{\mathrm{Colour}} \otimes \mathbb{1}_{\mathrm{Flavour}} S_F(p+q)S_F(p)\right] \\
&= N_f N_c \int \frac{d^4p}{(2\pi)^4} \, \mathrm{tr}\left[\mathbb{1}_{\mathrm{Dirac}} S_F(p+q)S_F(p)\right] \\
&= N_f N_c \int \frac{d^4p}{(2\pi)^4} \, \mathrm{tr}\left[\frac{(\not{p} + \not{q} + M)}{\left((p+q)^2 - M^2 + i\epsilon\right)} \frac{(\not{p} + M)}{\left(p^2 - M^2 + i\epsilon\right)}\right].
\end{aligned}
\tag{A.5}
$$

Since the trace is vanishing for arbitrary $\not{a}$ we get

$$-i\Pi_\sigma(q^2) = N_f N_c \int \frac{d^4p}{(2\pi)^4} \, \mathrm{tr}\left[\frac{\not{p}^2 + \not{q}\not{p} + M^2}{\left((p+q)^2 - M^2 + i\epsilon\right)\left(p^2 - M^2 + i\epsilon\right)}\right]. \tag{A.6}$$

Making use of the relation $\mathrm{tr}(\not{a}\not{b}) = 4ab$ yields

$$
\begin{aligned}
-i\Pi_\sigma &= 4N_f N_c \int \frac{d^4p}{(2\pi)^4} \left(\frac{p^2 + pq + M^2}{\left((p+q)^2 - M^2 + i\epsilon\right)\left(p^2 - M^2 + i\epsilon\right)}\right) \\
&= 4N_f N_c \int \frac{d^4p}{(2\pi)^4} \left(\frac{1}{\left(p^2 - M^2 + i\epsilon\right)} - \frac{pq + q^2 - 2M^2}{\left((p+q)^2 - M^2 + i\epsilon\right)\left(p^2 - M^2 + i\epsilon\right)}\right).
\end{aligned}
\tag{A.7}
$$

Now consider the following integral

$$
\int \frac{d^4p}{(2\pi)^4} \frac{2pq + q^2}{\left((p+q)^2 - M^2 + i\epsilon\right)\left(p^2 - M^2 + i\epsilon\right)}
$$

$$
\overset{p'=p+\frac{q}{2}}{=} \int \frac{d^4p'}{(2\pi)^4} \frac{2(p'-\frac{q}{2})q + q^2}{\left((p'+\frac{q}{2})^2 - M^2 + i\epsilon\right)\left((p'-\frac{q}{2})^2 - M^2 + i\epsilon\right)}
$$

$$
= \int \frac{d^4p'}{(2\pi)^4} \frac{2p'q}{\left((p'+\frac{q}{2})^2 - M^2 + i\epsilon\right)\left((p'-\frac{q}{2})^2 - M^2 + i\epsilon\right)} \tag{A.8}
$$

$$
\overset{p''=-p-\frac{q}{2}}{=} \int \frac{d^4p''}{(2\pi)^4} \frac{2(-p''-\frac{q}{2})q + q^2}{\left((-p''+\frac{q}{2})^2 - M^2 + i\epsilon\right)\left((-p''-\frac{q}{2})^2 - M^2 + i\epsilon\right)}
$$

$$
= \int \frac{d^4p''}{(2\pi)^4} \frac{-2p''q}{\left((p''+\frac{q}{2})^2 - M^2 + i\epsilon\right)\left((p''-\frac{q}{2})^2 - M^2 + i\epsilon\right)} . \tag{A.9}
$$

Comparing equation (A.8) with equation (A.9) yields

$$
\int \frac{d^4p}{(2\pi)^4} \frac{2pq + q^2}{\left((p+q)^2 - M^2 + i\epsilon\right)\left(p^2 - M^2 + i\epsilon\right)} = 0
$$

$$
\Longrightarrow \int \frac{d^4p}{(2\pi)^4} \frac{pq}{\left((p+q)^2 - M^2 + i\epsilon\right)\left(p^2 - M^2 + i\epsilon\right)} = \frac{d^4p}{(2\pi)^4} \frac{-\frac{q^2}{2}}{\left((p+q)^2 - M^2 + i\epsilon\right)\left(p^2 - M^2 + i\epsilon\right)} . \tag{A.10}
$$

Multiplying equation (A.7) with i and then inserting equation (A.10) yields

$$
\Pi_\sigma = 4iN_fN_c \int \frac{d^4p}{(2\pi)^4} \left(\frac{1}{\left(p^2 - M^2 + i\epsilon\right)} - \frac{\frac{q^2}{2} - 2M^2}{\left((p+q)^2 - M^2 + i\epsilon\right)\left(p^2 - M^2 + i\epsilon\right)} \right)
$$

$$
= 4iN_fN_c \int \frac{d^4p}{(2\pi)^4} \frac{1}{\left(p^2 - M^2 + i\epsilon\right)} - 2iN_fN_c \int \frac{d^4p}{(2\pi)^4} \frac{q^2 - 4M^2}{\left((p+q)^2 - M^2 + i\epsilon\right)\left(p^2 - M^2 + i\epsilon\right)}
$$

$$
= L_1 - \frac{L_2(q^2)}{2}\left(q^2 - 4M^2\right) . \tag{A.11}
$$

For the pion we obtain

$$
-i\Pi_\pi^{ab}(q^2) = -\int \frac{d^4p}{(2\pi)^4} \text{tr}\left[i\gamma_5 \otimes \mathbb{1}_{\text{Colour}} \otimes \tau^a i S_F(p+q) i\gamma_5 \otimes \mathbb{1}_{\text{Colour}} \otimes \tau^b i S_F(p) \right]
$$

$$
= -\delta_{ab} \int \frac{d^4p}{(2\pi)^4} \text{tr}\left[\gamma_5 S_F(p+q)\gamma_5 S_F(p) \otimes \mathbb{1}_{\text{Colour}} \otimes \mathbb{1}_{\text{Flavour}} \right]
$$

$$
= -\delta_{ab}N_fN_c \int \frac{d^4p}{(2\pi)^4} \text{tr}\left[\frac{\gamma_5(\slashed{p}+\slashed{q}+M)}{\left((p+q)^2 - M^2 + i\epsilon\right)} \frac{\gamma_5(\slashed{p}+M)}{\left(p^2 - M^2 + i\epsilon\right)} \right] . \tag{A.12}
$$

Using now $\{\gamma^5, \gamma^\mu\} = 0$ and $(\gamma_5)^2 = \mathbb{1}_{\text{Dirac}}$ gives

$$
-i\Pi_\pi^{ab}(q^2) = -\delta_{ab}N_fN_C \int \frac{d^4p}{(2\pi)^4} \text{tr}\left[\frac{(-\slashed{p}-\slashed{q}+M)(\slashed{p}+M)}{\left((p+q)^2 - M^2 + i\epsilon\right)\left(p^2 - M^2 + i\epsilon\right)} \right] . \tag{A.13}
$$

Now using again the relations $\text{tr}(\not{a}) = 0$ and $\text{tr}(\not{a}\not{b}) = 4ab$ lead to

$$-i\Pi_\pi^{ab}(q^2) = \delta_{ab}4N_f N_c \int \frac{d^4p}{(2\pi)^4}\left[\frac{p^2 + pq - M^2}{\left((p+q)^2 - M^2 + i\epsilon\right)\left(p^2 - M^2 + i\epsilon\right)}\right]$$

$$= \delta_{ab}4N_f N_c \int \frac{d^4p}{(2\pi)^4}\left[\frac{1}{\left(p^2 - M^2 + i\epsilon\right)} - \frac{pq + q^2}{\left(p^2 - M^2 + i\epsilon\right)\left((p+q)^2 - M^2 + i\epsilon\right)}\right]$$

(A.14)

Multiplying equation (A.14) with i and applying equation (A.10) yields

$$\Pi_\pi^{ab} = \delta_{ab}4iN_f N_c \int \frac{d^4p}{(2\pi)^4}\left[\frac{1}{\left(p^2 - M^2 + i\epsilon\right)} - \frac{\frac{q^2}{2}}{\left(p^2 - M^2 + i\epsilon\right)\left((p+q)^2 - M^2 + i\epsilon\right)}\right]$$

$$= \delta_{ab}\left(4iN_f N_c \int \frac{d^4p}{(2\pi)^4}\frac{1}{\left(p^2 - M^2 + i\epsilon\right)} - 2iN_f N_c \int \frac{d^4p}{(2\pi)^4}\frac{q^2}{\left(p^2 - M^2 + i\epsilon\right)\left((p+q)^2 - M^2 + i\epsilon\right)}\right)$$

$$= \delta_{ab}\left(L_1 - \frac{1}{2}L_2(q^2)q^2\right).$$

(A.15)

Bibliography

[1] T. CHENG and L. LI, *Gauge Theory of Elementary Particle Physics*, Oxford University Press, 2000.

[2] J. GOLDSTONE, A. SALAM, and S. WEINBERG, *Phys. Rev.* **127**, 965 (1962).

[3] T. KUGO, *Eichtheorie*, Springer, 1997.

[4] S. CARIGNANO, *Inhomogeneous chiral symmetry breaking phases*, PhD thesis, Technische Universität Darmstadt, 2012.

[5] S. CARIGNANO, M. BUBALLA, and B.-J. SCHAEFER, *Phys. Rev.* **D90**, 014033 (2010).

[6] U. MOSEL, *Fields, Symmetries, and Quarks*, Springer, 1999.

[7] W. PAULI and F. VILLARS, *Rev. Mod. Phys.* **21**, 434 (1949).

[8] B.-J. SCHAEFER and J. WAMBACH, *Phys. Rev.* **D75**, 085015 (2007).

[9] B.-J. SCHAEFER and J. WAMBACH, *Nucl. Phys.* **A757**, 479 (2005).

[10] V. SKOKOV, B. FRIMAN, E. NAKANO, K. REDLICH, and B.-J. SCHAEFER, *Phys. Rev.* **D82**, 034029 (2010).

[11] S. MÖLLER, Pion-Pion Scattering and Shear Viscosity in the Nambu-Jona-Lasinio Model, Master's thesis, Technische Universität Darmstadt, 2013.